

Some Novel Features of Three Dimensional MagnetoHydroDynamic Plasma

G-MHD3D: DNS Code for 3D MHD Plasma Modelling

Rupak Mukherjee Rajaraman Ganesh Abhijit Sen

Institute for Plasma Research, HBNI, Gandhinagar, Gujarat, India

rupakmukherjee01@gmail.com

rupak@ipr.res.in

ganesh@ipr.res.in

abhijit@ipr.res.in

Princeton Plasma Physics Laboratory

12 November, 2018

Direct Numerical Simulation (DNS) study of 3D Single fluid MagnetoHydroDynamic equations have been carried out to explore

- 1 Nonlinear Coherent Oscillation - a energy oscillation between kinetic and magnetic modes. RM, R Ganesh, Abhijit Sen; arXiv:1811.00744
- 2 “Recurrence Phenomena” - a periodic reconstruction of initial flow of fluid & magnetic variables. RM, R Ganesh, Abhijit Sen; arXiv:1811.00754
- 3 “Dynamo Effect” - Mean and intermediate scale magnetic field generation from driven chaotic flows. [Ongoing]

- 1 Finite mode / Galerkin representation confirms nonlinear interaction of few modes.
- 2 Rayleigh Quotient determines criteria of recurrence. [Key Parameter: Initial Condition]
- 3 Parameter set for *fast* dynamo is explored [Key Parameters: Forcing amplitude (\vec{f}_0) & Driving scale (k_f)]

Direct Numerical Simulation (DNS) study of 3D Single fluid MagnetoHydroDynamic equations have been carried out to explore

- 1 Nonlinear Coherent Oscillation - a energy oscillation between kinetic and magnetic modes. RM, R Ganesh, Abhijit Sen; arXiv:1811.00744
- 2 “Recurrence Phenomena” - a periodic reconstruction of initial flow of fluid & magnetic variables. RM, R Ganesh, Abhijit Sen; arXiv:1811.00754
- 3 “Dynamo Effect” - Mean and intermediate scale magnetic field generation from driven chaotic flows. [Ongoing]

- 1 Finite mode / Galerkin representation confirms nonlinear interaction of few modes.
- 2 Rayleigh Quotient determines criteria of recurrence. [Key Parameter: Initial Condition]
- 3 Parameter set for *fast* dynamo is explored [Key Parameters: Forcing amplitude (\vec{f}_0) & Driving scale (k_f)]

Direct Numerical Simulation (DNS) study of 3D Single fluid MagnetoHydroDynamic equations have been carried out to explore

- 1 Nonlinear Coherent Oscillation - a energy oscillation between kinetic and magnetic modes. RM, R Ganesh, Abhijit Sen; arXiv:1811.00744
- 2 “Recurrence Phenomena” - a periodic reconstruction of initial flow of fluid & magnetic variables. RM, R Ganesh, Abhijit Sen; arXiv:1811.00754
- 3 “Dynamo Effect” - Mean and intermediate scale magnetic field generation from driven chaotic flows. [Ongoing]

- 1 Finite mode / Galerkin representation confirms nonlinear interaction of few modes.
- 2 Rayleigh Quotient determines criteria of recurrence. [Key Parameter: Initial Condition]
- 3 Parameter set for *fast* dynamo is explored [Key Parameters: Forcing amplitude (\vec{f}_0) & Driving scale (k_f)]

Single Fluid 3D-MHD equations evaluated by G-MHD3D

$$\frac{\partial \rho}{\partial t} + \vec{\nabla} \cdot (\rho \vec{u}) = 0$$

$$\frac{\partial(\rho \vec{u})}{\partial t} + \vec{\nabla} \cdot \left[\rho \vec{u} \otimes \vec{u} + P_{\text{tot}} \vec{\bar{I}} - \frac{1}{4\pi} \vec{B} \otimes \vec{B} - 2\nu \rho \vec{\bar{S}} \right] = \rho \vec{F}$$

$$\frac{\partial E}{\partial t} + \vec{\nabla} \cdot \left[(E + P_{\text{tot}}) \vec{u} - \frac{1}{4\pi} \vec{u} \cdot (\vec{B} \otimes \vec{B}) \right. \\ \left. \left[-2\nu \rho \vec{u} \cdot \vec{\bar{S}} - \frac{\eta}{4\pi} \vec{B} \times (\vec{\nabla} \times \vec{B}) \right] \right] = 0$$

$$\frac{\partial \vec{B}}{\partial t} + \vec{\nabla} \cdot (\vec{u} \otimes \vec{B} - \vec{B} \otimes \vec{u}) = \eta \nabla^2 \vec{B}$$

$$S_{ij} = \frac{1}{2}(\partial_i u_j + \partial_j u_i) - \frac{1}{3} \delta_{ij} \vec{\nabla} \cdot \vec{u}$$

$$P_{\text{tot}} = P_{\text{th}} + \frac{1}{8\pi} |\vec{B}|^2; \quad P_{\text{th}} = C_s^2 \rho$$

- Evaluates single fluid 3-D MagnetoHydroDynamic equations.
- Pseudo-spectral technique is more accurate and faster than standard finite difference methods. [*FFTW & cuFFT library*]
- Can handle effects arising due to weak compressibility.
- 3D Isosurface reconstruction is developed using *Mayavi*.
- Diagnostics viz. Energy spectra, Particle & Field Line tracer (*Cloud-In-Cell & Velocity Verlet scheme*), Poincare Section are developed. [*In collaboration with Vinod Saini, IPR*]
- GPU code optimisation is achieved with OpenACC and CUDA parallelisation. [*With Naga Vydyanathan, NVIDIA, India*]
- Multi-GPU parallelisation (for high resolution runs) with NV-Link is in progress to run on NVIDIA-DGX station. [*In collaboration with Naga Vydyanathan, NVIDIA, India*]

- Evaluates single fluid 3-D MagnetoHydroDynamic equations.
- Pseudo-spectral technique is more accurate and faster than standard finite difference methods. [*FFTW & cuFFT library*]
- Can handle effects arising due to weak compressibility.
- 3D Isosurface reconstruction is developed using *Mayavi*.
- Diagnostics viz. Energy spectra, Particle & Field Line tracer (*Cloud-In-Cell & Velocity Verlet scheme*), Poincare Section are developed. [*In collaboration with Vinod Saini, IPR*]
- GPU code optimisation is achieved with OpenACC and CUDA parallelisation. [*With Naga Vydyanathan, NVIDIA, India*]
- Multi-GPU parallelisation (for high resolution runs) with NV-Link is in progress to run on NVIDIA-DGX station. [*In collaboration with Naga Vydyanathan, NVIDIA, India*]

- Evaluates single fluid 3-D MagnetoHydroDynamic equations.
- Pseudo-spectral technique is more accurate and faster than standard finite difference methods. [FFTW & cuFFT library]
- Can handle effects arising due to weak compressibility.

- 3D Isosurface reconstruction is developed using Mayavi.
- Diagnostics viz. Energy spectra, Particle & Field Line tracer (Cloud-In-Cell & Velocity Verlet scheme), Poincare Section are developed. [In collaboration with Vinod Saini, IPR]

- GPU code optimisation is achieved with OpenACC and CUDA parallelisation. [With Naga Vydyanathan, NVIDIA, India]
- Multi-GPU parallelisation (for high resolution runs) with NV-Link is in progress to run on NVIDIA-DGX station. [In collaboration with Naga Vydyanathan, NVIDIA, India]

- Evaluates single fluid 3-D MagnetoHydroDynamic equations.
- Pseudo-spectral technique is more accurate and faster than standard finite difference methods. [*FFTW & cuFFT library*]
- Can handle effects arising due to weak compressibility.
- 3D Isosurface reconstruction is developed using *Mayavi*.
- Diagnostics viz. Energy spectra, Particle & Field Line tracer (*Cloud-In-Cell & Velocity Verlet scheme*), Poincare Section are developed. [*In collaboration with Vinod Saini, IPR*]
- GPU code optimisation is achieved with OpenACC and CUDA parallelisation. [*With Naga Vydyanathan, NVIDIA, India*]
- Multi-GPU parallelisation (for high resolution runs) with NV-Link is in progress to run on NVIDIA-DGX station. [*In collaboration with Naga Vydyanathan, NVIDIA, India*]

- Evaluates single fluid 3-D MagnetoHydroDynamic equations.
 - Pseudo-spectral technique is more accurate and faster than standard finite difference methods. [FFTW & cuFFT library]
 - Can handle effects arising due to weak compressibility.
- 3D Isosurface reconstruction is developed using Mayavi.
 - Diagnostics viz. Energy spectra, Particle & Field Line tracer (Cloud-In-Cell & Velocity Verlet scheme), Poincare Section are developed. [In collaboration with Vinod Saini, IPR]
- GPU code optimisation is achieved with OpenACC and CUDA parallelisation. [With Naga Vydyanathan, NVIDIA, India]
 - Multi-GPU parallelisation (for high resolution runs) with NV-Link is in progress to run on NVIDIA-DGX station.[In collaboration with Naga Vydyanathan, NVIDIA, India]

Nonlinear Coherent Oscillation

- Within the premise of Single fluid MHD, energy can cascade through both kinetic and magnetic channels simultaneously.
- With weak resistivity, MHD model predicts -
 - 1). irreversible conversion of magnetic energy into fluid kinetic energy (i.e. [reconnection](#)).
 - 2). conversion of kinetic energy into mean large scale magnetic field (i.e. [dynamo](#)).
- **Question:** For a given fluid type and magnetic field strength, are there fluid flow profiles which do neither?
- **Answer:** [Yes](#). For a wide range of initial flow speeds or Alfvén Mach number it is shown that the coherent nonlinear oscillation persist.

Nonlinear Coherent Oscillation

- Within the premise of Single fluid MHD, energy can cascade through both kinetic and magnetic channels simultaneously.
- With weak resistivity, MHD model predicts -
 - 1). irreversible conversion of magnetic energy into fluid kinetic energy (i.e. [reconnection](#)).
 - 2). conversion of kinetic energy into mean large scale magnetic field (i.e. [dynamo](#)).
- **Question:** For a given fluid type and magnetic field strength, are there fluid flow profiles which do neither?
- **Answer:** **Yes.** For a wide range of initial flow speeds or Alfvén Mach number it is shown that the coherent nonlinear oscillation persist.

Nonlinear Coherent Oscillation

- Within the premise of Single fluid MHD, energy can cascade through both kinetic and magnetic channels simultaneously.
- With weak resistivity, MHD model predicts -
 - 1). irreversible conversion of magnetic energy into fluid kinetic energy (i.e. [reconnection](#)).
 - 2). conversion of kinetic energy into mean large scale magnetic field (i.e. [dynamo](#)).
- **Question:** For a given fluid type and magnetic field strength, are there fluid flow profiles which do neither?
- **Answer:** [Yes](#). For a wide range of initial flow speeds or Alfvén Mach number it is shown that the coherent nonlinear oscillation persist.

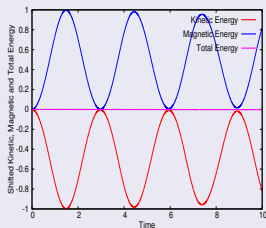
Nonlinear Coherent Oscillation

- Within the premise of Single fluid MHD, energy can cascade through both kinetic and magnetic channels simultaneously.
- With weak resistivity, MHD model predicts -
 - 1). irreversible conversion of magnetic energy into fluid kinetic energy (i.e. [reconnection](#)).
 - 2). conversion of kinetic energy into mean large scale magnetic field (i.e. [dynamo](#)).
- **Question:** For a given fluid type and magnetic field strength, are there fluid flow profiles which do neither?
- **Answer:** **Yes.** For a wide range of initial flow speeds or Alfvén Mach number it is shown that the coherent nonlinear oscillation persist.

Orszag-Tang Flow

$$u_x = -A \sin(k_0 y)$$

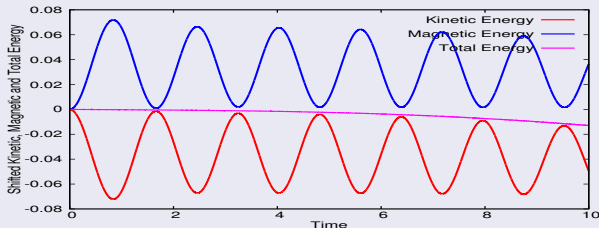
$$u_y = +A \sin(k_0 x)$$



Cat's Eye Flow

$$u_x = +\sin(k_0 x) \cos(k_0 y) - A \cos(k_0 x) \sin(k_0 y)$$

$$u_y = -\cos(k_0 x) \sin(k_0 y) + A \sin(k_0 x) \cos(k_0 y)$$

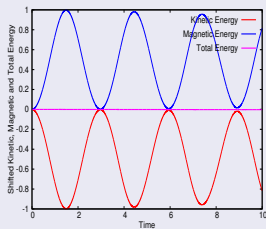


$$u_0 = \frac{L}{t_0}, \quad V_A = \frac{B_0}{4\pi\sqrt{\rho_0}}, \quad M_s = \frac{u_0}{C_s}, \quad M_A = \frac{u_0}{V_A}, \quad Re = \frac{\rho_0 u_0 L}{\nu}, \quad R_m = \frac{L u_0}{\eta}.$$

Orszag-Tang Flow

$$u_x = -A \sin(k_0 y)$$

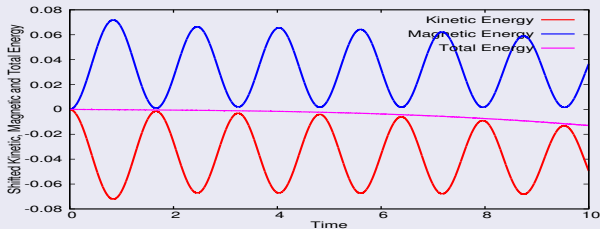
$$u_y = +A \sin(k_0 x)$$



Cat's Eye Flow

$$u_x = +\sin(k_0 x) \cos(k_0 y) - A \cos(k_0 x) \sin(k_0 y)$$

$$u_y = -\cos(k_0 x) \sin(k_0 y) + A \sin(k_0 x) \cos(k_0 y)$$



$$u_0 = \frac{L}{t_0}, \quad V_A = \frac{B_0}{4\pi\sqrt{\rho_0}}, \quad M_s = \frac{u_0}{C_s}, \quad M_A = \frac{u_0}{V_A}, \quad Re = \frac{\rho_0 u_0 L}{\nu}, \quad R_m = \frac{L u_0}{\eta}.$$

Nonlinear Coherent Oscillation at Alfvén Resonance (Sound speed = Alfvén speed) in 3D

Kinetic & magnetic energy for Roberts & TG flows.

Roberts flow:

$$u_x(0) = U_0 \sin(kz)$$

$$u_y(0) = U_0 \sin(kx)$$

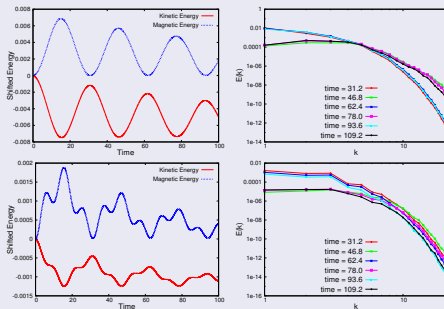
$$u_z(0) = U_0 \sin(ky)$$

Taylor-Green (TG) flow:

$$u_x(0) = A U_0 [\cos(kx) \sin(ky) \cos(kz)]$$

$$u_y(0) = -A U_0 [\sin(kx) \cos(ky) \cos(kz)]$$

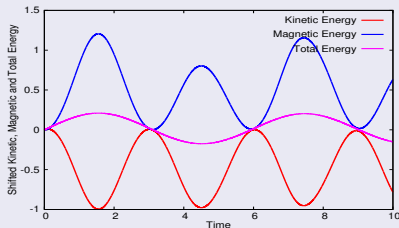
$$u_z(0) = 0$$



N	L	dt	ρ_0	U_0	Re	Rm	M_s	M_A	$A = B = C$	k_0
64^3	$2\pi^3$	10^{-5}	1	0.1	450	450	0.1	1	1	1

2D Orszag-Tang Flow with External Forcing

$$\vec{f} = \alpha \begin{bmatrix} -A \sin(k_f y) \\ +A \sin(k_f x) \end{bmatrix}, \quad \alpha = 0.1$$



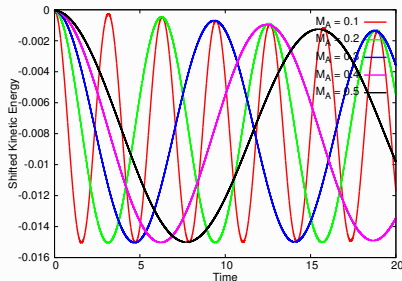
3D ABC Flow with different M_A

$$u_x = U_0[A \sin(k_0 z) + C \cos(k_0 y)]$$

$$u_y = U_0[B \sin(k_0 x) + A \cos(k_0 z)]$$

$$u_z = U_0[C \sin(k_0 y) + B \cos(k_0 x)]$$

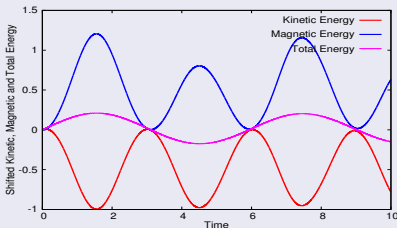
Frequency of energy exchange scales linearly with M_A .



- With external forcing similar to initial flow the plasma acts as a forced-relaxed system both in two and three dimensions.

2D Orszag-Tang Flow with External Forcing

$$\vec{f} = \alpha \begin{bmatrix} -A \sin(k_f y) \\ +A \sin(k_f x) \end{bmatrix}, \quad \alpha = 0.1$$



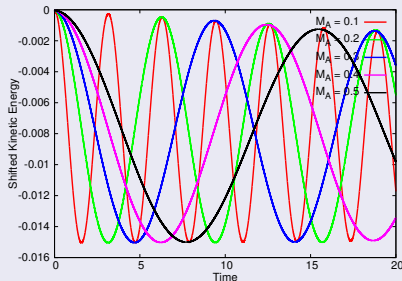
3D ABC Flow with different M_A

$$u_x = U_0[A \sin(k_0 z) + C \cos(k_0 y)]$$

$$u_y = U_0[B \sin(k_0 x) + A \cos(k_0 z)]$$

$$u_z = U_0[C \sin(k_0 y) + B \cos(k_0 x)]$$

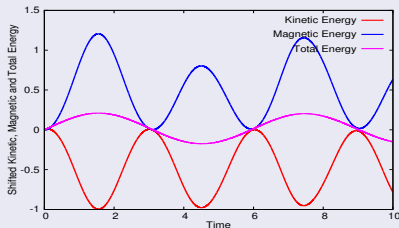
Frequency of energy exchange scales linearly with M_A .



- With external forcing similar to initial flow the plasma acts as a forced-relaxed system both in two and three dimensions.

2D Orszag-Tang Flow with External Forcing

$$\vec{f} = \alpha \begin{bmatrix} -A \sin(k_f y) \\ +A \sin(k_f x) \end{bmatrix}, \quad \alpha = 0.1$$



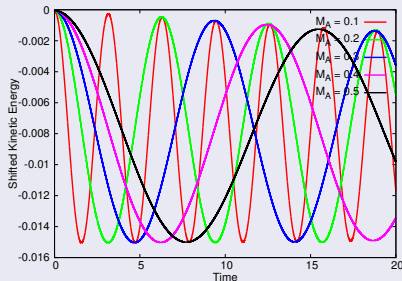
3D ABC Flow with different M_A

$$u_x = U_0[A \sin(k_0 z) + C \cos(k_0 y)]$$

$$u_y = U_0[B \sin(k_0 x) + A \cos(k_0 z)]$$

$$u_z = U_0[C \sin(k_0 y) + B \cos(k_0 x)]$$

Frequency of energy exchange scales linearly with M_A .

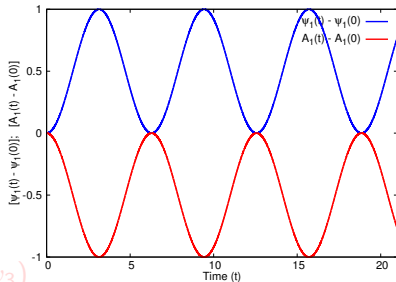


- With external forcing similar to initial flow the plasma acts as a forced-relaxed system both in two and three dimensions.

Galerkin representation of the field variables (stream function ψ ; vector potential A)

$$\psi(x, y) = \psi_0 \sin kx + e^{iky}(\psi_1 + \psi_3 \cos kx) + e^{-iky}(\psi_1^* + \psi_3^* \cos kx)$$

$$A(x, y) = A_0 \sin kx + e^{iky} (A_1 + A_3 \cos kx) + e^{-iky} (A_1^* + A_3^* \cos kx)$$



Initial Condition

Galerkin representation of the field variables (stream function ψ ; vector potential A)

$$\psi(x, y) = \psi_0 \sin kx + e^{iky} (\psi_1 + \psi_3 \cos kx) + e^{-iky} (\psi_1^* + \psi_3^* \cos kx)$$

$$A(x, y) = A_0 \sin kx + e^{iky} (A_1 + A_3 \cos kx) + e^{-iky} (A_1^* + A_3^* \cos kx)$$

$$\frac{d\psi_0}{dt} = ik^2(\psi_3^* \psi_1 - \psi_3 \psi_1^*)$$

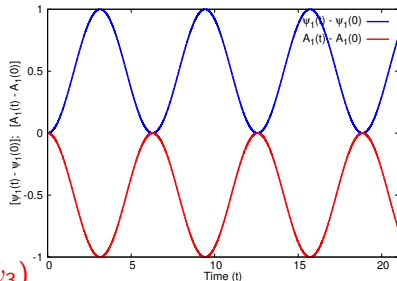
$$\frac{d\psi_1}{dt} = \frac{i}{2} k^2 (\psi_0 \psi_3 + A_0 A_3)$$

$$\frac{d\psi_3}{dt} = 0$$

$$\frac{dA_0}{dt} = ik^2 (A_3 \psi_1^* - A_3^* \psi_1 + A_1 \psi_3^* - A_1^* \psi_3)$$

$$\frac{dA_1}{dt} = \frac{i}{2} k^2 (A_0 \psi_3 - A_3 \psi_0)$$

$$\frac{dA_3}{dt} = ik^2 (A_0 \psi_1 - A_1 \psi_0)$$



Initial Condition

$$\psi_0 = 1, \psi_1 = 0 = \psi_3$$

$$A_0 = A_1 = A_3 = 1$$

RM, R Ganesh, Abhijit Sen, arXiv:1811.00744

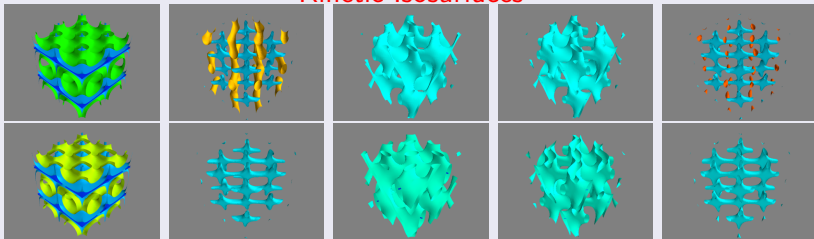
Summary of Nonlinear Coherent Oscillation

- For decaying flows at Alfvén resonance ($C_s = V_A$), an initial uniform magnetic field profile leads to nonlinear coherent oscillation between kinetic and magnetic modes.
- For externally driven flows, the nearly ideal magnetohydrodynamic plasma acts as a forced-relaxed system.
- The oscillation can be captured through a finite mode expansion of the MHD equations indicating the energy content is primarily in the large scales of the system.
- As the Alfvén Mach number is increased further, a tendency to mean field dynamo is seen.

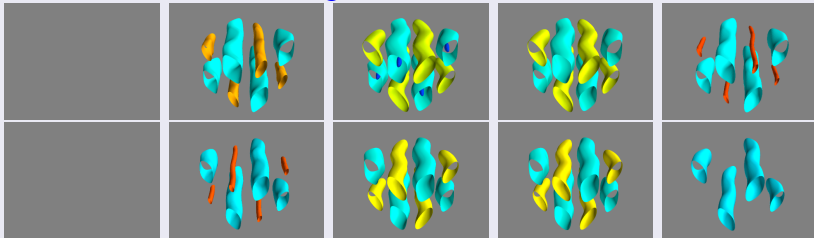
RECURRENCE in 3D MHD

- Reconstruction of initial condition in statistically large degrees of freedom systems - counterintuitive to laws of thermodynamics and entropy - trapping in phase space.
- Recurrence was first observed in 1D FPU system.
- In 2D hydrodynamic systems, reconstruction of initial flow field was numerically observed by Yen & Ferguson and explained by A Thyagaraja.
- However, generalising the analytical argument of recurrence in higher dimensional systems is quite challenging.
- We observe recurrence in single fluid 3D MHD system.
- We numerically extrapolate the previous analytical argument and find reasonable agreement with our DNS data.

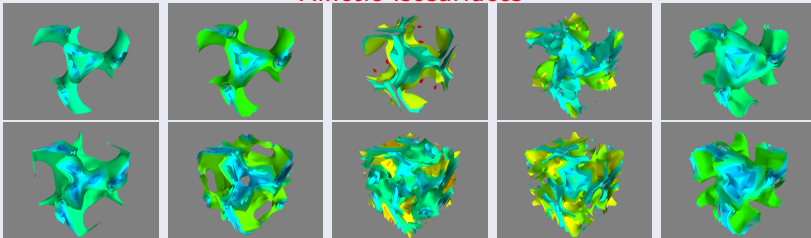
Kinetic Isosurfaces



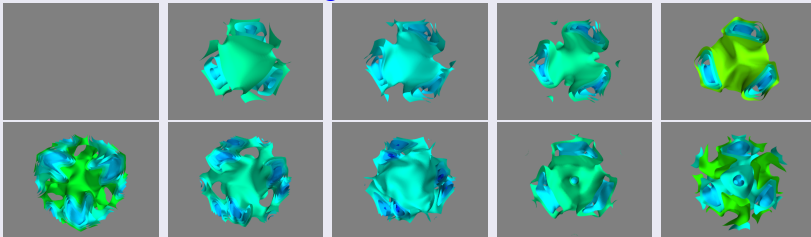
Magnetic Isosurfaces



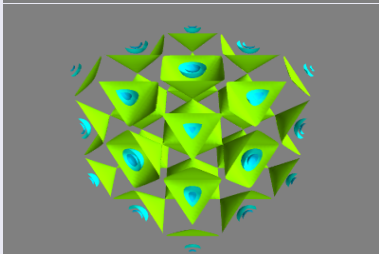
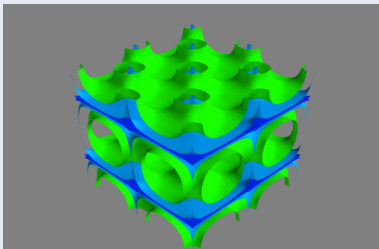
Kinetic Isosurfaces



Magnetic Isosurfaces



Recurrence for TG & Roberts flow



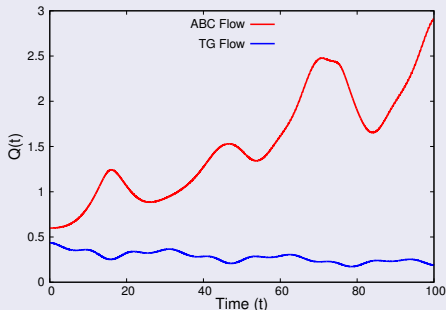
WHY DOES IT RECUR?

Rayleigh quotient

- Rayleigh quotient $[Q(t)]$ measures the number of effective **‘active degrees of freedom’**. [Thyagaraja, Phys. Fluids, 22 (11), 2093; Thyagaraja, Phys. Fluids, 24 (11), 1973]

$$Q(t) = \frac{\int_V \left[(\vec{\nabla} \times \vec{u})^2 + \frac{1}{2} (\vec{\nabla} \times \vec{B})^2 \right] dV}{\int_V \left(|\vec{u}|^2 + \frac{1}{2} |\vec{B}|^2 \right) dV} = \frac{\sum_k k^2 |c_k|^2}{\sum_k |c_k|^2} \text{ where, } \vec{u} \text{ \& \& } \vec{B} \text{ are expanded in a Fourier series.}$$

- If $Q(t)$ is bounded \Rightarrow Recurrence can happen.
- For TG & Roberts flow, $Q(t)$ is bounded.
- For ABC & Cats eye flow $Q(t)$ increases without bound.



RM, R Ganesh, Abhijit Sen,

arXiv:1811.00754

WHY DOES IT RECUR?

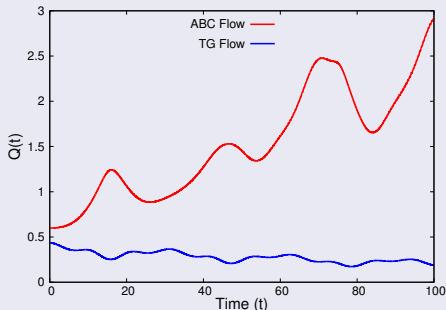
Rayleigh quotient

- Rayleigh quotient $[Q(t)]$ measures the number of effective **‘active degrees of freedom’**. [Thyagaraja, Phys. Fluids, 22 (11), 2093; Thyagaraja, Phys.

Fluids, 24 (11), 1973]

- $$Q(t) = \frac{\int_V \left[(\vec{\nabla} \times \vec{u})^2 + \frac{1}{2} (\vec{\nabla} \times \vec{B})^2 \right] dV}{\int_V \left(|\vec{u}|^2 + \frac{1}{2} |\vec{B}|^2 \right) dV} = \frac{\sum_k k^2 |c_k|^2}{\sum_k |c_k|^2}$$
 where, \vec{u} & \vec{B} are expanded in a Fourier series.

- If $Q(t)$ is bounded \Rightarrow Recurrence can happen.
- For TG & Roberts flow, $Q(t)$ is bounded.
- For ABC & Cats eye flow $Q(t)$ increases without bound.



RM, R Ganesh, Abhijit Sen,

arXiv:1811.00754

Summary of Recurrence

- Ideally very low probability of trapping in phase space in high dimensional systems (e.g. 3D MHD systems).
- Recurrence is observed for flows involving few number of **active** degrees of freedom. [Birkhoff, Dynamical Systems, 1927, Chapter 7]
- Generating the flows in experimental systems is achievable - hence can be tested in laboratory experiments.
- Recurrence can be helpful to make short time forecasts once typical initial profiles are experimentally obtained.
- Dissipative regularisation of 3D MHD discards Hamiltonian description leading to weak deviation from initial profiles.
- Conservative regularisation of 3D MHD [Thyagaraja, Phys Plasmas 17, 032503 (2010)] may offer better recurrence.

Introduction to Driven “self consistent” Dynamos

- Dynamo \Rightarrow Growth of magnetic energy at the cost of kinetic energy. [Mean field, Stretch-Twist-Fold (short scale) etc.] [Parker, ApJ, **122**, 293 (1955), Cowling, MNRAS, **94**, 39, (1933), Hotta, Science, **351**, 6280 (2016)]
- Work is in progress \Rightarrow Preliminary “fast” dynamo results.
- Results from 64^3 resolution runs. Higher resolution runs will be performed in multi-GPU code.
- It was shown by Alexakis, ABC field provides fastest kinematic dynamos [Phys Rev E, **84**, 026321 (2011)].
- We have tried to find optimised parameter set to obtain fast STF dynamos using ABC field.

Search for "fast" dynamo with externally driven ABC flow

- 'Self-consistent' dynamo saturates unlike kinematic dynamo.
- Linear growth rate (γ) increases with magnitude of forcing & k_f .
- Independent of initial condition.
- Multistep growth of magnetic energy.

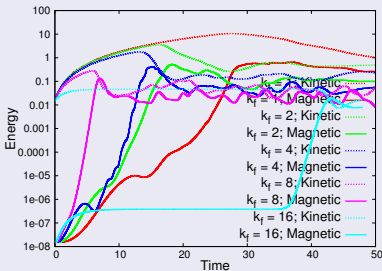
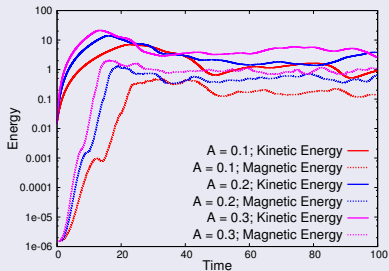
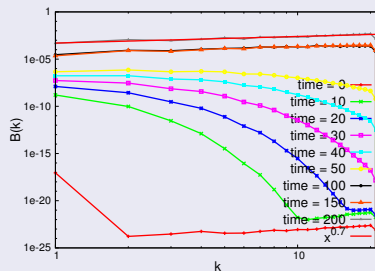
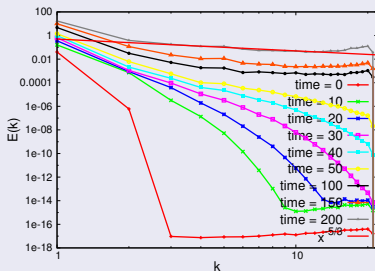


Figure: Saturation of self-consistent Dynamo action for different magnitude & wave-number of external forcing with parameters $N = 64^3$, $L = 2\pi^3$, $\delta t = 10^{-4}$, $\rho_0 = 1$, $U_0 = 0.1$, $M_A = 1000$, $M_s = 0.1$, $Re = Rm = 450$, $A = B = C = 0.1, 0.2, 0.3$ and $k_f = 1, 2, 4, 8, 16$ using MHD3D.

Kinetic and Magnetic Energy Spectra indicating STF dynamo

- Shell averaged kinetic energy spectra saturates with slope $-5/3$.
- Shell averaged magnetic energy spectra saturates with slope 0.7 .

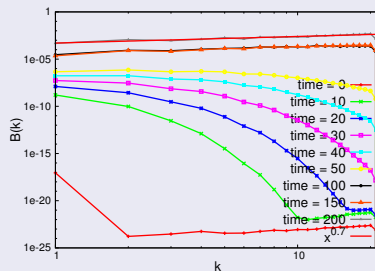
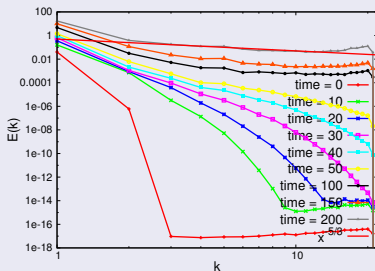


RM, R Ganesh, Abhijit Sen, Under preparation

- Preliminary energy spectra shows large and intermediate scales in magnetic variables are energetically dominant.
 - High resolution runs are needed to explore short scales.
- ⇒ Need for Multi-GPU G-MHD3D code.

Kinetic and Magnetic Energy Spectra indicating STF dynamo

- Shell averaged kinetic energy spectra saturates with slope $-5/3$.
- Shell averaged magnetic energy spectra saturates with slope 0.7 .



RM, R Ganesh, Abhijit Sen, Under preparation

- Preliminary energy spectra shows large and intermediate scales in magnetic variables are energetically dominant.
- High resolution runs are needed to explore short scales.
⇒ Need for Multi-GPU G-MHD3D code.

Summary & Discussions

- Coherent nonlinear oscillation between fluid and magnetic energies is numerically observed withing the framework of single fluid MagnetoHydroDynamics.
- Reconstruction of initial flow data is found to occur for 3D MHD system of equations. \Rightarrow [Recurrence](#)
- Fast dynamos are observed with chaotic flow lines at Prandtl number unity.

Acknowledgement

- A Thyagaraja, Culham Labs, UK
- Vinod Saini, Udaya Maurya, IPR, India
- Nagavijayalakshmi Vydyanathan, NVIDIA, India

Thank You

Summary & Discussions

- Coherent nonlinear oscillation between fluid and magnetic energies is numerically observed withing the framework of single fluid MagnetoHydroDynamics.
- Reconstruction of initial flow data is found to occur for 3D MHD system of equations. \Rightarrow [Recurrence](#)
- Fast dynamos are observed with chaotic flow lines at Prandtl number unity.

Acknowledgement

- A Thyagaraja, Culham Labs, UK
- Vinod Saini, Udaya Maurya, IPR, India
- Nagavijayalakshmi Vydyanathan, NVIDIA, India

Thank You

Summary & Discussions

- Coherent nonlinear oscillation between fluid and magnetic energies is numerically observed withing the framework of single fluid MagnetoHydroDynamics.
- Reconstruction of initial flow data is found to occur for 3D MHD system of equations. \Rightarrow [Recurrence](#)
- Fast dynamos are observed with chaotic flow lines at Prandtl number unity.

Acknowledgement

- A Thyagaraja, Culham Labs, UK
- Vinod Saini, Udaya Maurya, IPR, India
- Nagavijayalakshmi Vydyanathan, NVIDIA, India

Thank You

Motivation

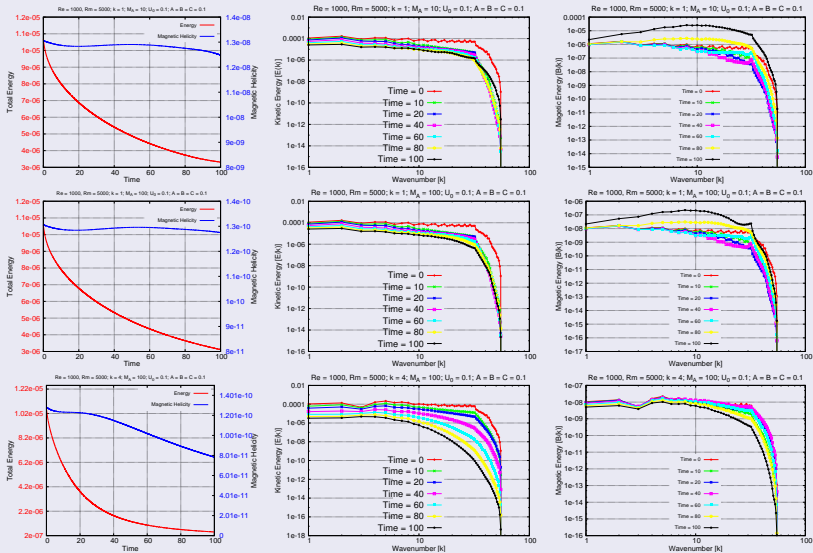
- A steady state for near ideal plasma was derived by L. Woltjer in 1954 by extremising the free energy constructed out of magnetic helicity ($H_m = \int \vec{A} \cdot \vec{B} dV$) and magnetic energy ($E_m = \int B^2 dV$ and $\vec{B} \cdot \hat{n} = 0$).
- This particularly yielded $\vec{\nabla} \times \vec{B} = \alpha(x)\vec{B}$ subject to $\vec{B} \cdot \vec{\nabla} \alpha = 0$ on the “walls”. $\alpha = \alpha(x)$ represents the rigidity of large number of volume ($H_m = \int_V \vec{A} \cdot \vec{B} dV$).
- J. B. Taylor considered a particular limit where, a weak dissipation would break all the local helicity constants except the one considered over the vessel with conducting surfaces, resulting in $\alpha(x) = \alpha_0 = \text{constant}$ and thereby, $\vec{\nabla} \times \vec{B} = \alpha_0 \vec{B}$.
- Thus it was known that large scales do not participate in the plasma relaxation until H. Qin *et al* [PRL, 109, 235001 (2012)] who has given arbitrary scale relaxation model.

Preliminary Numerical Experiment: Taylor - Woltjer / Qin

- We numerically evolve a three dimensional MHD plasma from a Beltrami class of solution in a region bounded by conducting walls ($\vec{B} \cdot \hat{n} = 0 = \vec{u} \cdot \hat{n}$) and “suddenly” allow to expand the plasma and fill the new volume.
- The expansion mediates via reconnection of magnetic field lines thereby flow of kin and mag energy between scales.
- We measure the scales involved during this relaxation of the plasma and from our numerical tools attempt to identify a model of plasma relaxation.

References

- Taylor, PRL, 33, 1139 (1974), Woltjer, PNAS, 44, 489 (1958)
- H Qin *et al*, PRL, 109, 235001 (2012)



Preliminary Results

- 1 The parameters chosen are such that magnetic helicity (H_m) remains constant while H_G decays allowing a Taylor-like situation.
- 2 For wavenumber $k = 1$, for all values of the parameters studies, power in magnetic energy spectra is seen to increase while the power in kinetic energy spectra decreases with time.
- 3 For $k = 4, 8$, the behavior is opposite for \vec{B} spectra.
- 4 As plasma expands from time $t = 0$ with $k = 1$ from a small volume to fill up the simulation volume, in general while the whole spectra is seen to contribute, mode numbers $k \sim 10$ are seen to participate in the relaxation process more dominantly.
- 5 For $k = 4, 8$, the relaxation process is dominantly controlled by $k > 10$ modes.

$$\frac{\partial \rho}{\partial t} + \vec{\nabla} \cdot (\rho \vec{u}) = 0$$

$$\vec{j} = \frac{1}{4\pi} \vec{\nabla} \times \vec{B}$$

$$\vec{E} = -\frac{\vec{u} \times \vec{B}}{c} + \eta \vec{j}$$

$$\frac{\partial \vec{u}}{\partial t} + (\vec{u} \cdot \vec{\nabla}) \vec{u} = \frac{\mu}{\rho} \nabla^2 \vec{u} - \frac{1}{\rho} \vec{\nabla} P + \frac{1}{\rho} (\vec{j} \times \vec{B})$$

$$\frac{\partial \vec{B}}{\partial t} = -c \vec{\nabla} \times \vec{E}$$

$$\vec{\nabla} \cdot \vec{B} = 0$$

$$\frac{d}{dt} \left(\frac{P}{\rho^\gamma} \right) = 0$$

$$\begin{aligned}
 \vec{\nabla} \times \vec{E} &= -\frac{1}{c} \vec{\nabla} \times (\vec{u} \times \vec{B}) + \vec{\nabla} \times (\eta \vec{j}) \\
 &= -\frac{1}{c} \vec{\nabla} \times (\vec{u} \times \vec{B}) + \frac{\eta}{4\pi} \vec{\nabla} \times (\vec{\nabla} \times \vec{B}) \\
 &= -\frac{1}{c} \vec{\nabla} \times (\vec{u} \times \vec{B}) + \frac{\eta}{4\pi} \nabla^2 \vec{B} \quad [\vec{\nabla} \cdot \vec{B} = 0] \\
 \vec{\nabla} \times (\vec{u} \times \vec{B}) &= (\vec{B} \cdot \vec{\nabla}) \vec{u} - (\vec{u} \cdot \vec{\nabla}) \vec{B} + \vec{u} (\vec{\nabla} \cdot \vec{B}) - \vec{B} (\vec{\nabla} \cdot \vec{u})
 \end{aligned}$$

Assumptions :

$$P = \gamma \rho K T \Rightarrow \frac{d}{dt} \left(\frac{P}{\rho^\gamma} \right) \equiv 0 \quad \text{identically}$$

$$\eta = 0$$

Definition :

$$M_A = \frac{U_0}{V_A} = \frac{|\vec{U}_0| \sqrt{4\pi\rho}}{|\vec{B}|}$$

Vector Identities : $(\vec{A} \times \vec{B}) \times \vec{C} = -\vec{C} \times (\vec{A} \times \vec{B})$

$$\vec{A} \times (\vec{\nabla} \times \vec{B}) + \vec{B} \times (\vec{\nabla} \times \vec{A}) = \\ \vec{\nabla}(\vec{A} \cdot \vec{B}) - (\vec{A} \cdot \vec{\nabla})\vec{B} - (\vec{B} \cdot \vec{\nabla})\vec{A}$$

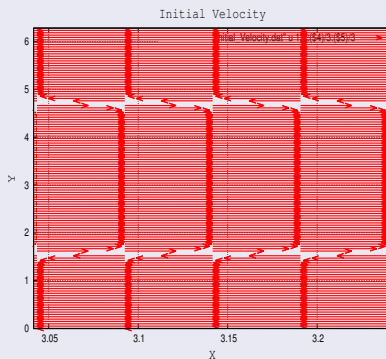
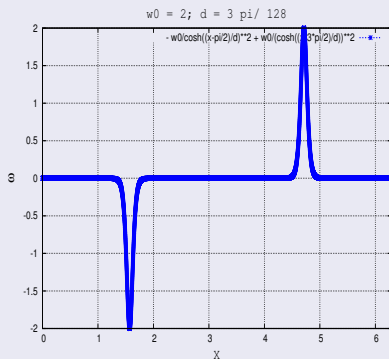
$$\Rightarrow \vec{B} \times (\vec{\nabla} \times \vec{B}) + \vec{B} \times (\vec{\nabla} \times \vec{B}) = \vec{\nabla}(\vec{B} \cdot \vec{B}) - (\vec{B} \cdot \vec{\nabla})\vec{B} - (\vec{B} \cdot \vec{\nabla})\vec{B}$$

$$\Rightarrow 2\vec{B} \times (\vec{\nabla} \times \vec{B}) = \vec{\nabla}(\vec{B}^2) - 2(\vec{B} \cdot \vec{\nabla})\vec{B}$$

$$\Rightarrow \vec{B} \times (\vec{\nabla} \times \vec{B}) = \frac{1}{2}\vec{\nabla}(\vec{B}^2) - (\vec{B} \cdot \vec{\nabla})\vec{B}$$

$$\Rightarrow (\vec{\nabla} \times \vec{B}) \times \vec{B} = (\vec{B} \cdot \vec{\nabla})\vec{B} - \frac{1}{2}\vec{\nabla}(\vec{B}^2)$$

Initial Condition: Kelvin-Helmholtz flow



- $\nu = 0.0001$

KH Instability with Tracer Particles (C-I-C & VV scheme)

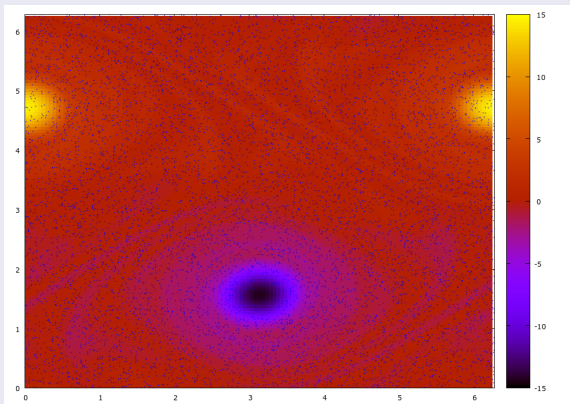


Figure: KH Instability for Incompressible Flow

Benchmarking with Analytical result

Analytical Growth Rate for a Broken Jet

Drazin, P. (1961). Journal of Fluid Mechanics, 10: 571-583.

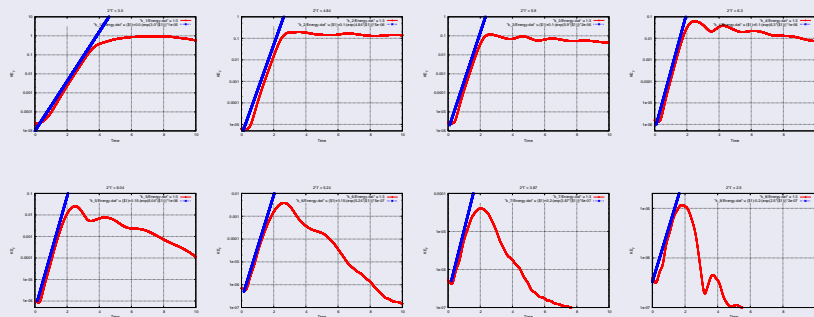
$$\gamma = \frac{k_x U_0}{3} \left[\sqrt{3} - 2 \frac{k_x}{R_E} - 2 \left\{ \left(\frac{k_x}{R_E} \right)^2 + 2\sqrt{3} \frac{k_x}{R_E} \right\}^{\frac{1}{2}} \right]$$

$$R_E = \frac{U_0 d}{\nu}$$

d = Shearing Length

Evaluation of Growth rate of KH Instability

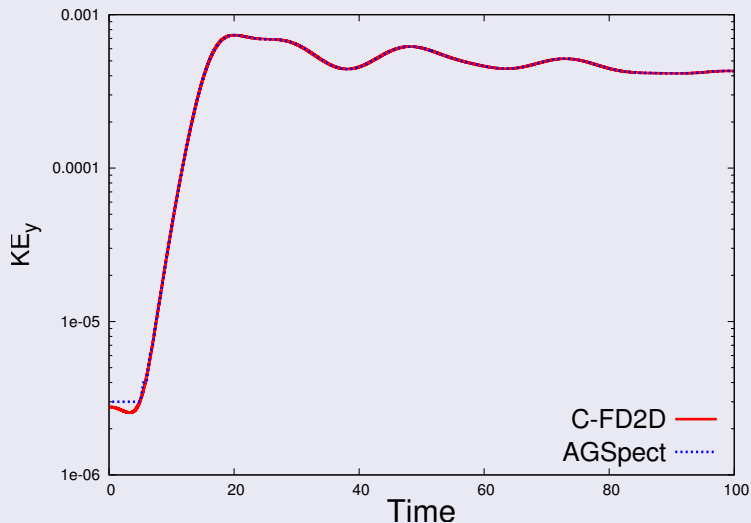
Numerical Growth Rate



- $L_x = L_y = 2\pi$; $\omega_0 = 25$; $d = \frac{3\pi}{128}$; $\nu = 0.0015$

Benchmark of MHD2D: Hydrodynamic (KH)

Growth Rate Comparison of KH with AGSpect; $k = 3$



Growth Rate with Mach Number

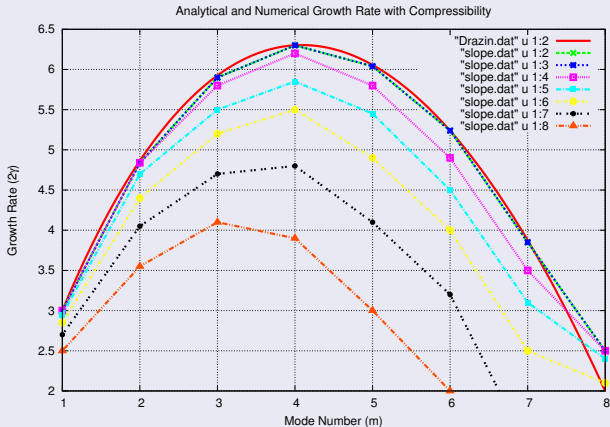


Figure: Analytical & $M = 0, 0.05, 0.1, 0.2, 0.3, 0.4, 0.5$

Benchmarking of MHD2D for compressible flows

Growth Rate at Large Mach Number: $M = 0.5$

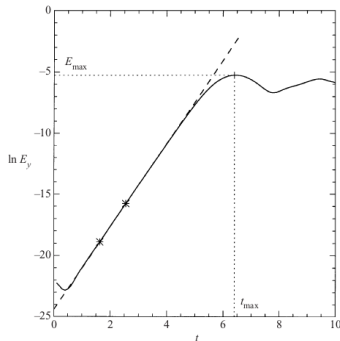
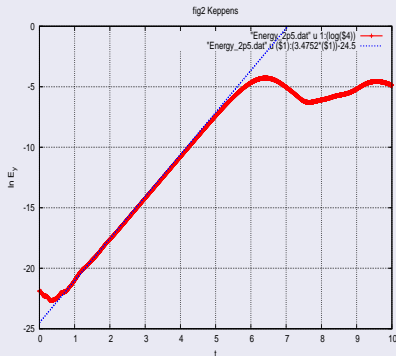


Figure: Benchmarked with R Keppens *et. al.*, JPP, **61** (1999)

Benchmarking of compressible MHD flows

Growth Rate at Large Mach Number: $M = 0.5$

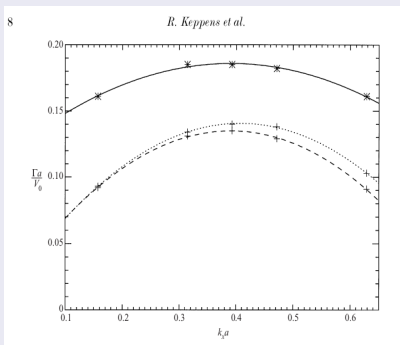
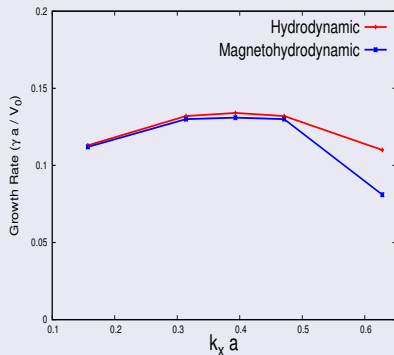
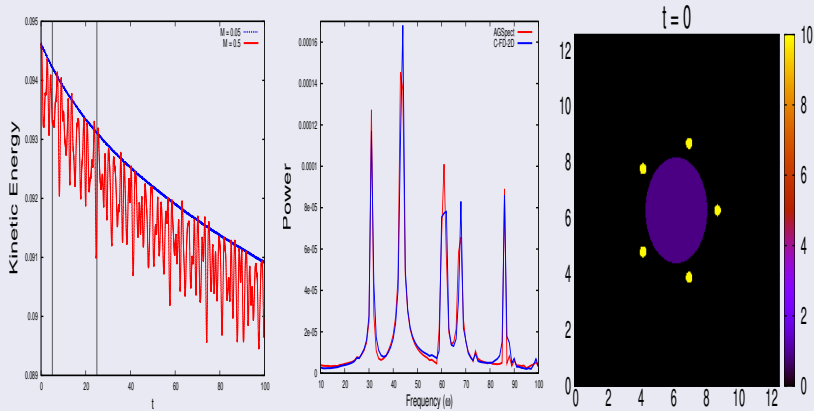


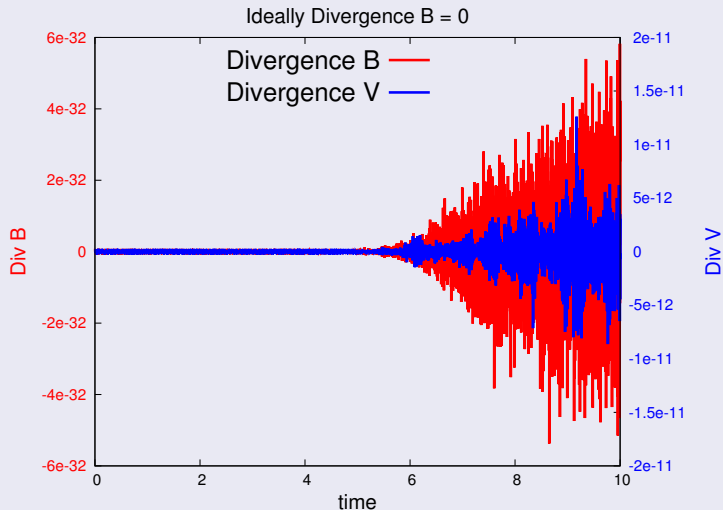
Figure: Benchmarked with R Keppens *et. al.*, JPP, **61** (1999)

Benchmarking of MHD2D for compressible flows

For compressible Vortex Merger Problem with AGSpect



$$\vec{\nabla} \cdot \vec{B} = 0 = \vec{\nabla} \cdot \vec{u}$$



GPU Performance of G-MHD3D (With Nagavijayalakshmi Vydyanathan, NVIDIA, India)

